A novel interface for cortical columnar neuromodulation with multi-point infrared neural stimulation

Fei-Yan Tian[1,2], Ying Zhang[1,2], Kenneth E. Schriver[1,3], Jia-Ming Hu[1,3*], Anna W. Roe[1,2,3,4*]

[1]Department of Neurosurgery of the Second Affiliated Hospital, Interdisciplinary Institute of Neuroscience and Technology, Zhejiang University, Hangzhou 310029, China

[2]Key Laboratory for Biomedical Engineering of Ministry of Education, College of Biomedical Engineering and Instrument Science, Zhejiang University, Hangzhou 310027, China

[3]MOE Frontier Science Center for Brain Science and Brain-machine Integration, School of Brain Science and Brain Medicine, Zhejiang University, Hangzhou, 310012, China

[4]National Key Laboratory of Brain and Computer Intelligence, Zhejiang University, Hangzhou 310058, China

*Corresponding author
Email: hujiaming@zju.edu.cn, or annawang@zju.edu.cn

Abstract

Cutting edge advances in electrical visual cortical prosthetics (VCPs) have evoked perception of shapes, motion, and letters in human and nonhuman primates. However, there is no existing method that employs a targeted columnar approach with a non-penetrating array of stimulation points. Neither has there been a direct demonstration that higher order cortical response can be elicited from externally stimulated lower order cortical sites. Here, we take an approach that employs images maps of cortical columns combined with delivery of optical stimulation through a fiber optic array to stimulate selected sets of columns. Specifically, using infrared neural stimulation (INS) delivered through a linear optic fiber array in anesthetized cat visual cortex, we predicted that the orientation of the array would selectively activate different higher order orientation domains in contralateral cat area 18. We found that INS modulation of response to ongoing visual oriented gratings produced enhanced responses in orientation-matched domains and reduced response in non-matched domains, consistent with a known higher order integration mediated by callosal inputs. This establishes proof-of-principle that an external device can access existing cortical circuitry via a column-targeted approach, and provides groundwork for a targeted column-based approach to cortical prosthetics using dense optical fiber bundle arrays.

Keywords: infrared neural stimulation, orientation-selective response, neuromodulation, fiber optic array, brain-machine interface, visual cortex

Main text

Introduction

Developing visual cortical prosthetics (VCPs) for the blind (and those with low vision and other vision deficits) has long been a driving force behind vision research. From the days of Dobelle[1], to current advanced studies in humans and monkeys, groundbreaking work has demonstrated that electrical stimulation delivered through multicontact arrays can elicit perception of shapes, motion, and letters[2,3]. Advances in electrode technology and stimulation methods have brought significant quantitative and qualitative advances to VCPs. With low to moderate stimulation currents, Utah arrays are now able to evoke perception of fine shapes and features[4,5]. Development of 'current steering' methods in humans demonstrated enhanced saliency of evoked percepts over static stimulation patterns[6]. Evidence from studies in monkeys show that focal low current electrical stimulation of cortex can modulate featurally specific percepts. These include single site stimulation of (1) direction domains in MT to modulate perception of the direction of a field of moving dots (Salzmann & Newsome[7]), (2) disparity tuned (near-to-far) sites in MT to bias depth perception (DeAngelis and colleagues[8]), and (3) presumed color sites in V1 to modulate the visibility of a small color spot in a background color matching task (Tehovnik[3], in humans, see Schmidt et al[9]). Stimulation of face patches in temporal cortex led to non-specific distorted face percepts, perhaps due to the higher electrical current range used (50-300uA)[10]. Studies that have employed electrical (Friedman[11], Card[12], Hu[13]), optogenetic (Chernov[14], Zaraza[15]), and infrared (Cayce[16], Xu[17]) neural stimulation to stimulate single cortical columns lead to activation of local functionally matched orientation and color domain networks, further suggesting that single site stimulation impacts a larger network of functionally selective response. Together, these examples support the hypothesis that the lower stimulation intensities have minimal current spread, allowing selective stimulation of single cortical columns and their associated networks, resulting in perceptual modulation related to the column-encoded feature.

Columnar organization of visual cortex. The columnar organization of visual cortex has long been known and provides a beautiful roadmap for accessing different featural loci underlying perception. In visual cortex of humans, monkeys, and carnivores, different cortical areas have distinct spatial layouts representing, for example, features of color, contour orientation, motion, and depth. While previous VCP studies have stimulated to single functional columns[18] and have recognized the importance of incorporating cortical circuitry in VCP design, technologies were not available to map the submillimeter-sized columns organization of visual cortex (in humans ~500 μm[19,20]; monkeys ~200-300 μm[21], cat ~500 μm[22]). Now, with the development of ultrahigh field MRI and high resolution imaging methods, it becomes feasible to obtain columnar maps for targeted stimulation[20,23]. Another important aspect of columnar organization is that, from area to area, information from 'lower order' columns are integrated in 'higher order' columns in downstream areas, thereby establishing de novo parameter spaces. A columnar VCP must therefore be capable of targeting desired sets of columns, and, ideally, with knowledge of the downstream effects. Here, we conduct a proof of principle demonstration of a column-targeted approach and show that higher order representations can be predictably activated by columnar stimulation.

Technological approach. To enable selective stimulation of sets of cortical columns, our approach is to employ a non-penetrating optical stimulation method (called infrared neural stimulation, INS, 1875±10 nm)[24] delivered through an array of multiple fibers[25]. Optical arrays can be designed to match the size and density

of cortical columns and can be placed on cortical windows in different positions and can be removed when not in use. INS stimulates brain tissue via brief pulses of heat which induces membrane capacitance change and subsequent neuronal activation[26]. Within the parameters used, it is non-damaging to tissue[24,27,28] and requires no prior viral transfection, making it amenable for use in cats, primates and humans[16,17,29,30] (Supplementary materials). Applications in humans have begun[29] (clinical trials for peripheral nerve stimulation and cochlear stimulation: Jansen, Richter). Similar to electrical[2,5] and optogenetic stimulation[31,32] in nonhuman primates, application of INS to primate visual cortex elicits phosphenes to which the animal saccades[24]. Using fiber optics of appropriate size (200 μm), we have shown that stimulation leads to focal activation of functionally specific columns and their associated columnar networks within V1[13,14,16,33]. That is, stim of single columns leads to enhancement of nearby columns. However, unknown is whether stimulation of multiple columns in an area can lead to higher order response in another area.

Higher order orientation in cat area 18. Previous studies have shown that, similar to area V2 in macaque monkeys, cat area 18 is responsive to illusory contours (**Figure 1**A)[34] and that one of the sources of illusory contour response are the callosal connections[35] (Figure 1B, upper schematic). Here, we have designed a 5 optical fiber array to target cortical columns in cat visual area 18 and used optical imaging to monitor the contralateral cortex in response to array stimulation placed in one of two orientations (Figure 1B, bottom). The stimulator is apposed to the cortex without penetration, and can be moved to different locations on the brain. We show that this interface enables focal, column-based INS stimulation and activates predicted higher order orientation-selective effects in contralateral area 18. This demonstrates an interface that can activate native columnar organizations and their associated circuits, and provides promise for a targeted, column-based VCP.

Results

Hypothesis

Our stimulation paradigm derives from psychophysical studies in which adding a visual cue can accentuate or reduce the perception of a scene (e.g., cross orientation suppression[36]). Based on previous studies[37], we predict that adding a 'vertical' cue can bias the cortical response towards vertical and away from horizontal. We had previously shown that stimulating a single orientation domain leads to enhancement of connected 'like' orientation domains and relative suppression of 'orthogonal' orientation domains[13,14]. However, whether stimulating multiple sites can induce higher order responses is unknown.

Our testbed for this question is area 17 and 18 of cat visual cortex, areas whose topographic organization, functional orientation domain organization, and callosal connectivity is well known[35,38–41]. Callosal projections arise from cells near the 17/18 border and axons terminate broadly in multiple cortical columns over several square millimeters of contralateral cortex[40]. These non-topographic projections also project in a bilaminar pattern avoiding layer 4, supporting an interaction that generates higher order response[35]. Pulsed INS stimulation is known to effectively activate the superficial layers[16,17], where callosally projecting neurons reside[40]. To address the modulatory effect of array stimulation, we tested whether stimulation of linear points on the cortex (which is known to activate neurons in cat visual cortex area 18 sensitive to the orientation of the stimulated points) would evoke differential effects on domains

with matching vs non-matching orientation preference. As illustrated in Figure 1C and 1D, visual presentation of a vertical grating evokes a response (Figure 1E, green line, a negative reflectance change detected by intrinsic signal imaging, see Methods) in vertical orientation domains (Figure 1D, blue domains), while the horizontal grating evokes a response (Figure 1F, green line) in horizontal orientation domains (Figure 1D, peach domains). We predicted that adding a line of INS stimulation (Figure 1D, red asterisks) parallel to the vertical meridian (VM, which is represented at the 17/18 border) will enhance the response of vertical domains (Figure 1E, black line, downwards red arrow indicates greater reflectance change than vision alone), and will suppress the horizontal domain response (Figure 1F, black line, upwards red arrow, reduction of reflectance change).

Mapping 17/18 Border, Focal Stimulation, and Intensity Dependence

We begin by identifying the border between areas 17 (cat V1) and 18 (cat V2) bilaterally (**Figure 2**A-C). Optical imaging (OI) establishes orientation maps in response to drifting gratings (0° vs. 90°) in area 17 (prefers higher spatial frequency and lower temporal frequency gratings) and area 18 (prefers lower spatial frequency and higher temporal frequency gratings) on both sides (Figure 2B and 2C)[42,43]. From this, the border between areas 17 and 18 is determined[42] (yellow dashed line), which is a 1-1.5-mm-wide zone of cytoarchitectonic transition rather than a sharp border[44]. The border represents the vertical meridian (VM), and guides the placement of the optical fiber array in a 'vertical' orientation (parallel to the VM) or in a horizontal orientation (roughly orthogonal to the VM).

We also demonstrate that INS stimulation achieves focal submillimeter-sized activations and intensity dependent activation. As shown in Figure 2D, single fiber INS stimulation (from 0.3-0.7 $J\cdot cm^{-2}$) applied to the surface of cat visual cortex induces an intensity-dependent response (Figure 2E and 2F). The mean activation sizes for radiant exposures 0.3$J\cdot cm^{-2}$, 0.5$J\cdot cm^{-2}$, 0.7$J\cdot cm^{-2}$ are 240μm, 350μm, and 420μm respectively (Figure 2G, red dots). This is well within the ~500 μm size of cat orientation domains and indicates that INS can stimulate orientation domains selectively[16].

Single and Multi-Fiber Stimulation: Modulation of Contralateral Orientation Networks

We now ask whether INS coupled with visually evoked activity can be used to modulate a range of cortical responses. Such modulation would potentially make INS an important and useful tool to enhance cortical response under natural sensory and behavioral conditions. Our experimental configuration combining OI, visual stimulation, and multi-fiber INS is shown schematically in **Figure 3**A. Experimental conditions are shown in Figure 3B.

Single Fiber Stimulation (Figure 3B, Single): We first investigated whether each single optical fiber evoked a local response. Although each fiber is calibrated at the beginning of the experiment to deliver the same radiant exposure ($J\cdot cm^{-2}$), we further confirmed this by assessing the similarity of cortical response (OI spatial size and amplitude of reflectance change) across fibers. **Figure 4**A highlights five fibers evaluated in one experiment (colored arrows). The results of INS at each fiber tip at 0.3 $J\cdot cm^{-2}$ (without visual stimulation) are shown in Figure 4D (INS activation maps). The activations were focal, submillimeter in size (diameter within 0.5mm), and similar to activations evoked by visual spot stimulations (**Figure S4**)[45]. Moreover, the locations of the activations shifted in topographic sequence, similar to the sequence of

activations induced by a moving dot[46,47]. Thus, the activations of single fibers within the array were focal and topographic, indicating the suitability of using single fibers in sequence to mimic a moving point stimulus. The time course curves of the reflectance change for each fiber are shown in Figure 4B. These are typical INS induced time course curves, peaking 1-1.5s following stimulation onset followed by a gradual return to baseline. Figure 4C shows the amplitudes of OI response are similar (mean dR/R = -0.07%) across fibers. These single fiber tests were conducted at the beginning of each experiment to confirm that comparable stimulations were delivered by the fibers in the array.

Sequential Multi-Fiber Stimulation (Figure 3B, Slow Fwd, Slow Rev, Fast Fwd, Fast Rev, Random): Previous studies have shown that a linearly moving dot can evoke the sensation of an oriented contour[48]. To mimic this, we delivered INS across five collinear points in area 18 (at 0.3 $J \cdot cm^{-2}$); the effect of two speeds and two directions on oriented visual stimulation was examined. As shown in Figure 1, we expected to see enhancement of response in orientation-selective domains matched to that of the fiber array orientation, and reduction in response of orientation-selective domains orthogonal to the fiber array orientation. We also investigated whether the direction of the INS sequence affected the response of the orientation-selective domains.

As shown in **Figure 5** (Cat 2), we combined sequential 'vertical' array stimulation (Figure 5A, array parallel to VM in cat area 18), with vertical (Figure 5B) and horizontal (Figure 5C) visual grating stimulation. Orientation maps derived from each of these combined 'vision+INS' stimulations were compared to 'vision only' orientation maps. In addition, the vertical array conditions comprised two directions and two speeds (slow: 2mm cortical distance/s, fast: 24mm/s; similar to a dot moving at 3 deg/s and ~36 deg/s, respectively). As a control, a non-directional 'random' array stimulus (which induces a much weaker vertical percept) was added (see Figure 3B). All 13 conditions were randomly interleaved within each trial and each trial was repeated 15 times.

Figure 5B and 5C show, for each condition, the time course of the intrinsic signal reflectance changes for vertical and horizontal orientation-selective domains, respectively. All conditions show responses that peak around 2.5 – 3.5 s after stimulation onset with peak magnitudes ranging from 0.1 to 0.3%, typical of OI signals. Figure 5B shows that vertical visual stimulation alone (green trace) produced a peak response amplitude of ~0.15%, and that adding vertical INS (as shown in Figure 5A) to visual vertical stimulation resulted in an enhanced (~0.05%, downwards red arrow) response in vertical domains (Figure 5B, brown: slow, black: fast). In contrast, adding vertical INS to visual horizontal stimulation led to a reduction (~0.1%, upwards red arrow) in response (Figure 5C, brown: slow, black: fast). This differential effect is quantified in Figure 5D (vertical domains, Welch's t-test, $p < 0.001$ for all comparisons, except vision alone vs. vision + random INS ($p < 0.01$)) and 5E (horizontal domains, Welch's t-test, $p < 0.001$ for all comparisons). The effect of single directions of INS stimulation also produced similar orientation-matched enhancement and non-matched reduction of the same trend (**Figure S1**). No significant difference was observed between slow and fast INS. Addition of random INS stimulation to visual stimulation resulted in reduction in response to both vertical (~0.05%) and horizontal (~0.15%) orientation domains (Figure 5B, 5C magenta; Figure 5D, 5E last column), suggesting that the scattered incoherent flashes interfere with contour orientation response. We also note that fiber tip locations spanned multiple different orientation domains (Figure 5A, from anterior to posterior, estimated to be 90°,0°,135°,100°,20°), so the contour orientation effect is not a result of INS

stimulation of vertical orientation domains in the left hemisphere, but rather, we infer, a result of topographic multipoint integration.

In another case (Cat 3) we placed the linear fiber array approximately orthogonal to the VM ("horizontal INS") as shown in **Figure 6**A. Eleven of the 13 conditions in case 1 were investigated (random stimulation was not used in this experiment); each trial was repeated 10 times. Here, the results largely mirrored those observed in Cat 2. Sequential horizontal INS suppressed OI response in the vertical orientation-selective domains at both fast and slow speeds (Figure 6B, black and brown traces). The response of horizontal orientation-selective domains was enhanced by slow INS stimulation (Figure 6C, brown trace), but fast INS stimulation resulted in no significant change (Figure 6C, black trace) compared to visual stimulation alone (green trace). The effect is further quantified in Figure 6D (vertical domains, Welch's t-test, $p < 0.001$) and 6E (horizontal domains, Welch's t-test, $p < 0.001$ between vision alone and vision + slow INS).

We also examined the effects of higher stimulation intensity. Previous studies have shown that increasing stimulation intensity can bias the excitatory/inhibitory balance such that a general suppression is invoked[49]. Our results of adding a higher intensity INS stimulation (0.7 $J \cdot cm^{-2}$) to visual stimulation revealed relative suppression of all conditions. These results are shown in **Figure 7**. All experimental parameters were the same as described above except that the radiant energy was increased to 0.7 $J \cdot cm^{-2}$. Under these higher fluence conditions, we observed a reduction in the OI reflectance signal irrespective of the orientation of the fiber optic array, the direction of INS stimulation, or the speed of INS stimulation. Suppressive effects ranged from ~0.05% to ~0.1%, and the effect is further quantified in Figure 7 (Welch's t-test).

Discussion

We summarize key aspects of this visual brain-machine interface:

(1) Columnar stimulation: As assessed by OI of cortical response, we found that single fiber activation was confined to single <0.5mm loci (Figure 2 and 4), well within the size of cat orientation columns[22]. Because feature parameters are represented at mesoscale and are intermixed locally (e.g. different orientation columns within a 1-2 mm-sized region), BMI electrical stimulation of >1mm loci activates multiple types of feature nodes near the stimulation tip, leading to a non-specific 'phosphene-like' experience. As we have demonstrated here, an optical stimulation approach can provide spatially specific effects (diameter of activation size within 500μm), expanding possibilities for selectively interfacing with column-based features[25]. With lower stimulation intensities, it is feasible to reach even smaller activation sizes (Figure 2G).

(2) Neuromodulation: Inducing a percept by adding external stimulation to an ongoing elevated baseline can have enhancing or inhibiting effects[50]. Here, we have combined a linear arrangement of stimulation points to ongoing visual oriented gratings, demonstrating an enhancement when the stimulation effect is matched to the orientation of the visual stimulus and a relative suppression when not matched. These orientation-specific effects were seen with both 'slow' and 'fast' array stimulation (Figure 5; except at high INS intensities in Figure 7), consistent with the breadth of velocity preferences in cat area 18[51]. Orthogonal placement of the INS array on the cortex resulted in symmetrically opposite effects, as predicted (Figure 6). Random sequences of INS stimulation, which does not induce a salient 'moving dot' percept

failed to induce this oriented effect and in fact led to a general reduction of signal (Figure 5). Previous studies on intracortical circuitry have shown stimulation of single orientation domains in cat area 18 lead to relative enhancement (suppression) of connected matched (non-matched) orientation domains in area 18[13]. For callosal circuits, as Makarov 2008 showed[35], there are circuits in the carnivore brain that underlie this type of orientation-selective cross-callosal integration. They concluded that the schematic (Figure 1B, upper) is the likely circuit. Our demonstration that a VCP can induce the same integrated orientation-selective (enhancement: matched, relative suppression: non-matched) response suggests that it activates the same circuits. Thus, our data suggest that INS applied to cortical columns can predictably access the circuits underlying higher order orientation response.

(3) Dynamics: The ideal brain-machine interface for enhancing vision would be able to deliver time-varying stimuli for eliciting distinct perceptual effects. Here, using a single five fiber array, we presented 10 stimulation paradigms: stimulation of single fibers, sequential five-fiber stimulation in two directions and at two speeds, and random (non-directional) five-fiber stimulation. Similar capabilities have been developed in other studies[6,52].

(4) Higher order response: For each oriented placement of the fiber array on the cortex, our linear array fiber tip locations targeted different orientation domains in one hemisphere (Figure 5 and 6) and achieved selective activation in the contralateral hemisphere. Random sequences did not produce this result. We showed that the contralateral orientation-specific response, despite receiving inputs from multiple different orientations, resulted from topographic multipoint integration. While previous VCP studies have induced oriented and motion[53] percepts from multisite stimulation[34,37,54–57], we suggest that it is possible to achieve smaller (e.g. <1º) percepts for finer detail vision. Future application of INS stimulation in behaving monkeys will evaluate this possibility.

(5) Linking the contralateral visual hemifield. This study highlights an approach for linking the two visual hemifields[58]. We find that not only are there responses induced in the contralateral hemisphere, but that they are integrated in way to achieve orientation-domain specific effects. Callosal connections are important for integrating the left and right visual fields (e.g. for reading[59],), tying together the vertical meridian[60–62], and the fovea (which is represented on both hemispheres[63]). These aspects of vision and visually guided behaviors are also challenges that must be addressed by VCPs.

(6) Intensity dependence and general suppression: Effects were intensity-dependent: weak effects were seen at 0.1 $J \cdot cm^{-2}$; a clear modulating effect was observed at 0.3 $J \cdot cm^{-2}$, and at higher intensities of 0.7 $J \cdot cm^{-2}$, a general suppression of response was observed, consistent with other reports of suppression at higher INS intensities[16,64,65]. As shown by multiple previous studies[66], such intensity-dependence is an important element of developing a reliable VCP.

(7) Limitations: While fiber optic designs can cause less tissue damage when used for cortical surface stimulation and can be placed on different locations on the brain, the array must be removed when not in use, limiting its capacity for use in freely behaving monkey studies; however, in the future, it may be possible to engineer a μ-LED stimulation design that is wireless[15,67–69]. A major limitation of fiber optic arrays compared to electrode array interfaces is that they are unable to, alone, record neuronal spike activity. While our design does incorporate neural signals via OI or fMRI, for direct spiking activity, neural recordings

can be conducted in a separate session of column-targeted electrical recording. In addition, unlike optogenetics, INS is not cell type specific, a limitation that could be overcome by conducting column targeted optogenetic stimulation through windows on the brain[14,70]. To increase flexibility of stimulation patterns, we have developed a 100-fiber bundle array and have applied this to cortex in anesthetized monkeys, with plans to do so in awake monkeys[25,71]. Note that deep brain stimulators may also be designed[72,73].

Previous studies with electrical stimulation

Evidence from previous studies using electrical stimulation suggest that selective stimulation of cortex evokes featurally specific percepts. While the specific parameters of different studies vary (intensity, frequency, duration), we summarize a few studies that potentially achieved column-specific stimulation be employing relatively low stimulation intensities. Salzmann & Newsome[7] showed that a monkey's direction discrimination of a moving dot field is biased towards the preferred direction of the electrically stimulated (10μA in 1s) column. Similarly, in the disparity axis, DeAngelis and colleagues[8] showed that stimulating (20μA) patches of cells with selective disparity tuning in MT resulted in a perceptual bias towards the stimulated near-to-far column's disparity preference. In a carefully conducted study in which visibility of a small color spot was eliminated by presenting a matching background color, the equivalent electrical stimulation (15-55μA) needed to achieve a similar effect was identified, illustrating that stimulation of V1 sites elicited unsaturated color percepts[3]. In humans, Schmidt et al[9] showed that stimulating with low current levels near threshold (e.g. 1.9μA) in ventral temporal cortex, percepts of color were often evoked and that increasing stimulation led to more washed out color percepts such as white, gray, or yellow (consistent with the blurring of signals across multiple functional domains). Stimulation of face patches in temporal cortex led to non-specific distorted face percepts, perhaps due to the higher electrical current range used (50-300μA)[10]. Thus, together, these examples may support the hypothesis that stimulation of a single cortical column or patch can, with the lower stimulation intensities, lead to a perception related to the column-encoded feature. Further investigation is needed.

Given the percepts induced by single site stimulation, what can be elicited by multisite stimulation? A few studies have examined the percepts evoked by multisite electrical stimulation, either sequentially[1,5,6,52] or simultaneously[4,5]. In human studies, surface electrodes (0.5-3mm diameter, impedance <18kΩ, stimulation frequency 60/120/200 Hz, and current amplitudes 0.3-4/1.2-1.5 mA, several millimeters spacing, spanning a few centimeters in V1 and V2, over 10º of visual space) have evoked percepts of shapes and letters. These percepts can be enhanced by a 'dynamic current steering' stimulation paradigm[6], enhancing the salience of the percept and reducing the number of stimulation sites needed[52,74]. In a study by Fernández et al.[4], a blind subject implanted with a Utah array was able to discriminate evoked sizes and shapes as well as spatially small percepts, marking a significant advance in spatial resolution (see also Yoshor and Bosking[75]). Roelfsema's group implanted an astounding 1024-channel-count electrode interface (16 Utah arrays, 0.3-0.6MΩ, <100uA) into monkey V1 and V4, achieving percepts of shapes, letters, and motion direction[5]. Although presumably higher order circuits associated with these sites of stimulation were activated, the associated brain circuits were not studied.

VCP activates known circuitry for generating higher order visual processing facilitated by callosal

connection. Thus far, in VCP research there has been little emphasis on callosal function. In both cats and monkeys, callosal connections link similar topographic locations at or near the vertical meridian. The callosal fibers in essence stitch together the two halves of the visual field[76]. In addition to linking topographically matched points, callosal connections also mediate integration of inputs from the contralateral hemisphere to achieve a higher order functional integration (e.g. higher orientation). This type of integration serves to link and emphasize the information at the vertical meridian. This type of integration and known overrepresentation of vertical is hypothesized to underlie perceptual enhancements at the vertical meridian[77]. As evidenced by studies in split brain patients, callosal function is a critical aspect of vision that needs to be addressed in VCPs. There are also studies that indicate callosal interactions are important for binocular vision[78].

In our VCP design, we aimed to target known functional columns in visual cortex and predicted the resulting activation based on known circuitry. We find that our results are quite consistent with previous studies. In a study in the ferret (carnivore with similar visual cortical organization[79]) which recorded local field potentials during presentation of grating stimuli, removal of inputs from one hemisphere by cooling revealed a primary excitation between orientation-matched neurons and a secondary suppression between orthogonally oriented neurons[35]. Here, we find that stimulation through a linear array produced enhanced response in higher order orientation domains matching that of the array and suppressed responses from orthogonal higher order domains. As proposed by Makarov[35], this integration is likely mediated via integration in contralateral area 18 (Figure 1B, upper). Thus, we show that external activation is capable of activating callosal circuits in a manner very similar to visual stimulation. This demonstration supports the possibility that externally applied focal stimulation can access functional circuitry known to underlie normal visual perception.

In addition, our previous research[24] suggested that INS applied to visual cortex induces visual phosphenes, leading to predicted saccade behavior in the awake, behaving monkey. These findings demonstrate feasibility for INS to be used as a cortical stimulation method that can be incorporated into visual cortical prosthetics. Combined with our aim of targeting cortical columns, we aim to enhance or restore spatially and featurally specific visual percepts.

Materials and Methods

Animal Procedures

All procedures were in compliance with and approved by the Institutional Animal Care and Use Committee of Zhejiang University and followed the guidelines of the National Institutes of Health Guide for the Care and Use of Laboratory Animals. Experiments were performed in hemispheres of ten cats (weighing 3-4kg). Three animals were used to develop the stimulation procedure, 2 animals to acquire intensity dependence data, and 5 animals to obtain the INS/vision combined data. For surgical procedures, cats were sedated with ketamine hydrochloride (10mg/kg)/atropine (0.03mg/kg) and anesthetized with isoflurane (1.5-2%)[17]. Animals were intubated and artificially ventilated. End-tidal CO_2, respiration rate, SpO_2, heart rate, and electrocardiogram were monitored and maintained. Temperature (37.5-38.5°C) was monitored and maintained via a circulating water blanket. A craniotomy (Horsley-Clarke coordinates A10-P5, L7-R7) and durotomy ware performed to expose visual cortex areas 17 and 18 of both hemispheres. A

piece of transparent acrylic sheet, with an opening for insertion of a linear fiber array, was placed on top of the cortex to suppress physiological motion. After the stabilization of cortex, for acquisition of functional neural signals in the brain, cats were anesthetized with propofol (induction 5mg/kg, maintenance 5-10mg/kg/h, i.v.) and isoflurane (~0.5%). To prevent the movement of the eyes, a muscle relaxant was used (vecuronium bromide, induction 0.25mg/kg, maintenance 0.05-0.1mg/kg/h, i.v.). EEG was monitored to ensure the maintenance of sleep spindles consistent with anesthesia level-2 used in human neurosurgery. The pupils were dilated with atropine sulfate (1%) and the nictitating membranes were retracted with neosynephrine (5%). The eyes were corrected with appropriate contact lenses to focus on a monitor 57cm in front of the animal. At the end of data collection, the animal was overdosed with pentobarbital sodium (100mg/kg, i.v.).

Visual stimuli

Visual stimuli were created using ViSaGe (Cambridge Research Systems Ltd) and presented on a monitor refreshed at 60Hz and positioned 57cm from the cat's eyes. Visual stimuli were presented binocularly. Full screen drifting square gratings were used to obtain orientation maps in visual cortical area 18 (0.2 cycle/degree, 5 Hz) and area 17 (0.5 cycle/degree, 2 Hz). Bidirectionally moving gratings were presented in a randomly interleaved fashion in 1 of 2 orientations (vertical, horizontal).

Intrinsic Signal Optical Imaging

Imaging was performed with Imager 3001 (Optical Imaging Inc., Israel). Images were obtained from the CCD camera (1308 x 1080 pixels, 10.8 x 8.7 mm) with 630 nm illumination. Frames were acquired at 4Hz for 4s or 5s and were synchronized to respiration. Visual stimuli were presented to obtain orientation maps and determine the border of area 17/18. Each condition was presented for 20-30 trials, pseudo-randomly interleaved with at least a 7s intertrial interval. A blood vessel map of the cortex (Figure 2A) was also acquired under 570 nm illumination for analysis.

Infrared Neural Stimulation

We stimulated using an 1870 nm infrared pulsed laser (Changchun New Industries Optoelectronics, FC-W-1870nm-4W, China), coupled to an optical switch (Piezo Jena AG, Germany) and then to a multi-channel linear fiber array (200μm diameter per fiber, 500μm fiber spacing) (Figure 3A). The fiber array was carefully positioned with a 3D-manipulator (RWD, China, stereotaxic micromanipulator), guided by the optical imaging camera mounted directly above the region of interest (shown as Figure 2A-C), the angle between the fiber and cortical surface was around 45°, and the fiber tips were just in contact with the cortex. The maximum output power of the laser device at 200Hz frequency is 200mW and the output power can be adjusted. Before each experiment, a power meter (Thorlabs, USA, PM320E, with thermal power sensor: S401C) is used to measure the output energy from the fiber tip, to ensure that the peak energy density (radiant exposure) of the laser pulse at the tip of the fiber reaches the value we need, such as 0.3 or 0.7 $J \cdot cm^{-2}$ (18.84 or 43.96 mW), calculation formula:

$$\text{Power} = \text{radiant exposure} \times \text{area} \times \text{pulse repetition frequency} \quad (1)$$

The pulse generator (Master-9, Israel) continuously generated an output signal of 200 Hz (INS

stimulation frequency). Then, Arduino control board (Italy) can be programmed to determine opening duration (16ms or 200ms) and order (sequential or random) of each channel of the optical switch. Due to the channel switching is controlled by the optical switch, while the laser device is always on during this process, the output power of the laser device is stable.

As shown in Figure 3B, we generated both fast and slow sequential INS stimulations (Fast: 200 ms per tip, Slow: 16 ms per tip); for each condition, the total duration of laser stimulation across all five tips was 1s. Each stimulation was also delivered in two directions (Fwd, Rev). The Slow and Fast conditions (200 ms per tip and the 16 ms per tip) are similar to a dot moving at ~3 deg per sec and ~30 deg per sec, respectively (typical velocity preference of cat area 18 ~25 deg per sec[51]). All INS was initiated 0.5 s after the onset of optical imaging data acquisition (t=0) and coincident with the onset of visual stimulation. Conditions were pseudo-randomly interleaved within each trial and repeated 15 times. Image acquisition was synchronized with respiration to reduce variability in OI reflectance signal.

INS imaging experiment comprised 13 conditions at a specific radiant exposure (0.3, 0.7 $J \cdot cm^{-2}$). These conditions contain: blank condition (no visual stimulation or INS); 2 INS off conditions with visual stimuli (vertical and horizontal grating orientations); and 10 INS on conditions, including two orientations, each paired with five different INS paradigms (two directions: forward, reverse; two speeds: slow, fast; and one rapidly, randomly changing stimulus) (see Figure 3B).

Data Analysis

Data analysis was performed with Matlab (The Mathworks, Matlab-R2021a). To obtain single condition maps, for each trial, the reflectance change of each pixel was calculated first using the functions: $dR/R = (F_X - F_0)/F_0$, where F_X is the reflectance value corresponding to frames X (X=1-20), F_0 is the average reflectance value of the first two frames (taken before laser or visual stimulation onset). To remove low-frequency noise (e.g., gradations in illumination across the cortex, slow 0.1Hz oscillations, slow physiological fluctuations), maps were low-pass filtered (Gaussian filter, 3-8 pixels diameter), and low-frequency noise was reduced by convolving the map with a 150-200 pixels diameter (~1.2-1.6 mm) circular filter and subtracted from the original maps[13]. For the imaging results, pixel values were clipped by mean ±1.5/2 standard deviation (SD) or mean ±0.05/0.1% values (e.g. **Fig. S2**B, values larger than mean +2 SD/0.05% was truncated to mean +2 SD/0.05%). These values were further used for calculating time courses.

Difference maps between two stimulus conditions (e.g. INS vs. blank or two orthogonal orientations) were obtained by calculating the average difference of filtered single condition maps. Maps were also clipped as described above. For INS only, maps were calculated from average of the fourth to the seventh frame (Figure 2D and 4D); for visual stimulation alone and combined visual stimulation and INS, frames 9-16 were used (Figure 2B, 2C, 5A and 6A). Based on our image acquisition frame rate (250 ms per frame), we observed initial activation at 250ms after INS onset (i.e., in the next frame to the stimulation onset).

We used two-tailed t-test for the comparison of the responses between two conditions (INS on vs. off, or two orthogonal orientations). Only regions with $p<0.001$ were selected for further analysis (e.g., right

panels in Figure 5A and 6A, **Figure S3**). Response time courses were obtained from these selected regions (See Figure 5B and 5C).

To estimate the activation size, we chose the areas where responses to INS stimuli were significantly stronger than the blank condition (two-tailed t-test, $p<0.001$). We manually drew the elliptical contour of the activation area, and measured the lengths of the long and short axes using Image J (1 pixel = 8 μm). The average value of the long and short axes was calculated as the diameter of the activation area.

Statistics

Prism (GraphPad Software, Prism 8) was used for statistical analysis. To test whether INS significantly modulates the cortical response to visual stimuli, after homogeneity of variance validation, a Welch's t-test was performed on averaged data (typically frames 10-20) to determine statistical significance between two conditions (INS on vs. off).

Acknowledgments

This work was supported by: STI 2030-Major Projects 2021ZD0200401(to A.W.R.), Key Research and Development Program of Zhejiang Province 2020C03004 (to A.W.R.), National Natural Science Foundation of China U20A20221, 819611280292 (to A.W.R.). We thank Xinjian Li and Rob Friedman for helpful comments.

Author Contributions: F.Y.T. and Y.Z. performed the experimental studies. F.Y.T. carried out the analysis. F.Y.T, K.E.S, J.M.H. and A.W.R wrote the manuscript. A.W.R. supervised the work and provided the funding.

Competing Interest Statement: The authors declare no competing interests.

References

1. Dobelle, W. H., Mladejovsky, M. G. & Girvin, J. P. Artificial Vision for the Blind: Electrical Stimulation of Visual Cortex Offers Hope for a Functional Prosthesis. *Science, New Series* **183**, 440–444 (1974).

2. Tehovnik, E. J., Slocum, W. M. & Schiller, P. H. Microstimulation of V1 delays the execution of visually guided saccades. *Eur J of Neuroscience* **20**, 264–272 (2004).

3. Schiller, P. H., Slocum, W. M., Kwak, M. C., Kendall, G. L. & Tehovnik, E. J. New methods devised specify the size and color of the spots monkeys see when striate cortex (area V1) is electrically stimulated. *Proc. Natl. Acad. Sci. U.S.A.* **108**, 17809–17814 (2011).

4. Fernández, E. *et al.* Visual percepts evoked with an intracortical 96-channel microelectrode array inserted in human occipital cortex. *Journal of Clinical Investigation* **131**, e151331 (2021).

5. Chen, X., Wang, F., Fernandez, E. & Roelfsema, P. R. Shape perception via a high-channel-count neuroprosthesis in monkey visual cortex. *Science* **370**, 1191–1196 (2020).

6. Beauchamp, M. S. *et al.* Dynamic Stimulation of Visual Cortex Produces Form Vision in Sighted and Blind Humans. *Cell* **181**, 774-783.e5 (2020).

7. Salzman, C., Murasugi, C., Britten, K. & Newsome, W. Microstimulation in visual area MT: effects on direction discrimination performance. *J. Neurosci.* **12**, 2331–2355 (1992).

8. DeAngelis, G. C., Cumming, B. G. & Newsome, W. T. Cortical area MT and the perception of stereoscopic depth. *Nature* **394**, 677–680 (1998).

9. Schmidt, E.M., Bak, M. J., Hambrecht, F. T., Kufta, C. V., O'Rourke, D. K. & Vallabhanath, P. Feasibility of a visual prosthesis for the blind based on intracorticai microstimulation of the visual cortex.

10. Moeller, S., Crapse, T., Chang, L. & Tsao, D. Y. The effect of face patch microstimulation on perception of faces and objects. *Nat Neurosci* **20**, 743–752 (2017).

11. Friedman, R. M., Morone, K. A., Gharbawie, O. A. & Roe, A. W. Mapping mesoscale cortical connectivity in monkey sensorimotor cortex with optical imaging and microstimulation. *J of Comparative Neurology* **528**, 3095–3107 (2020).

12. Card, N. S. & Gharbawie, O. A. Principles of Intrinsic Motor Cortex Connectivity in Primates. *J. Neurosci.* **40**, 4348–4362 (2020).

13. Hu, J. M., Qian, M. Z., Tanigawa, H., Song, X. M. & Roe, A. W. Focal Electrical Stimulation of Cortical Functional Networks. *Cerebral Cortex* **30**, 5532–5543 (2020).

14. Chernov, M. M., Friedman, R. M., Chen, G., Stoner, G. R. & Roe, A. W. Functionally specific optogenetic modulation in primate visual cortex. *Proc. Natl. Acad. Sci. U.S.A.* **115**, 10505–10510 (2018).

15. Zaraza, D. *et al.* Head-mounted optical imaging and optogenetic stimulation system for use in behaving primates. *Cell Reports Methods* **2**, 100351 (2022).

16. Cayce, J. M. *et al.* Infrared neural stimulation of primary visual cortex in non-human primates. *NeuroImage* **84**, 181–190 (2014).

17. Xu, A. G. *et al.* Focal infrared neural stimulation with high-field functional MRI: A rapid way to map mesoscale brain connectomes. *Sci Adv* **5**, eaau7046 (2019).

18. Christie, B. P., Ashmont, K. R., House, P. A. & Greger, B. Approaches to a cortical vision prosthesis: implications of electrode size and placement. *J. Neural Eng.* **13**, 025003 (2016).

19. Adams, D. L., Sincich, L. C. & Horton, J. C. Complete Pattern of Ocular Dominance Columns in Human Primary Visual Cortex. *J. Neurosci.* **27**, 10391–10403 (2007).

20. Yacoub, E., Harel, N. & Uğurbil, K. High-field fMRI unveils orientation columns in humans. *Proc. Natl. Acad. Sci. U.S.A.* **105**, 10607–10612 (2008).

21. Hubel, D. H. & Wiesel, T. N. Uniformity of monkey striate cortex: A parallel relationship between field size, scatter, and magnification factor. *J. Comp. Neurol.* **158**, 295–305 (1974).

22. Shmuel, A. & Grinvald, A. Functional Organization for Direction of Motion and Its Relationship to Orientation Maps in Cat Area 18. *J. Neurosci.* **16**, 6945–6964 (1996).

23. Cheng, K., Waggoner, R. A. & Tanaka, K. Human Ocular Dominance Columns as Revealed by High-Field Functional Magnetic Resonance Imaging. *Neuron* **32**, 359–374 (2001).

24. Chernov, M. & Roe, A. W. Infrared neural stimulation: a new stimulation tool for central nervous system applications. *Neurophoton* **1**, 011011 (2014).

25. Kim, S. *et al.* Whole-brain mapping of effective connectivity by fMRI with cortex-wide patterned

optogenetics. *Neuron* **111**, 1732-1747.e6 (2023).

26. Plaksin, M., Kimmel, E. & Shoham, S. Correspondence: Revisiting the theoretical cell membrane thermal capacitance response. *Nat Commun* **8**, 1431 (2017).
27. Thompson, A. C., Wade, S. A., Brown, W. G. A. & Stoddart, P. R. Modeling of light absorption in tissue during infrared neural stimulation. *J. Biomed. Opt* **17**, 0750021 (2012).
28. Thompson, A. C., Wade, S. A., Cadusch, P. J., Brown, W. G. A. & Stoddart, P. R. *J. Biomed. Opt* **18**, 035004 (2013).
29. Pan, L. *et al.* Infrared neural stimulation in human cerebral cortex. *Brain Stimulation* **16**, 418–430 (2023).
30. Matic, A. I. *et al.* Behavioral and Electrophysiological Responses Evoked by Chronic Infrared Neural Stimulation of the Cochlea. *PLoS ONE* **8**, e58189 (2013).
31. Gerits, A. *et al.* Optogenetically Induced Behavioral and Functional Network Changes in Primates. *Current Biology* **22**, 1722–1726 (2012).
32. Dai, J., Brooks, D. I. & Sheinberg, D. L. Optogenetic and Electrical Microstimulation Systematically Bias Visuospatial Choice in Primates. *Current Biology* **24**, 63–69 (2014).
33. Hu, J. M. & Roe, A. W. Functionally specific and sparse domain-based micro-networks in monkey V1 and V2. *Current Biology* **32**, 2797-2809.e3 (2022).
34. Gharat, A. & Baker, C. L. Motion-defined contour processing in the early visual cortex. *Journal of Neurophysiology* **108**, 1228–1243 (2012).
35. Makarov, V. A., Schmidt, K. E., Castellanos, N. P., Lopez-Aguado, L. & Innocenti, G. M. Stimulus-Dependent Interaction between the Visual Areas 17 and 18 of the 2 Hemispheres of the Ferret (Mustela putorius). *Cerebral Cortex* **18**, 1951–1960 (2008).

36. Brouwer, G. J. & Heeger, D. J. Cross-orientation suppression in human visual cortex. *Journal of Neurophysiology* **106**, 2108–2119 (2011).

37. Mather, G., Pavan, A., Bellacosa, R. M. & Casco, C. Psychophysical evidence for interactions between visual motion and form processing at the level of motion integrating receptive fields. *Neuropsychologia* **50**, 153–159 (2012).

38. Tusa, R. J., Rosenquist, A. C. & Palmer, L. A. Retinotopic organization of areas 18 and 19 in the cat. *J. Comp. Neurol.* **185**, 657–678 (1979).

39. Bonhoeffer, T., Kim, D.-S., Malonek, D., Shoham, D. & Grinvald, A. Optical Imaging of the Layout of Functional Domains in Area 17 and Across the Area 17/18 Border in Cat Visual Cortex. *European Journal of Neuroscience* **7**, 1973–1988 (1995).

40. Houzel, J.-C., Milleret, C. & Innocenti, G. Morphology of Callosal Axons Interconnecting Areas 17 and 18 of the Cat. *European Journal of Neuroscience* **6**, 898–917 (1994).

41. Matsubara, J., Cynader, M. & Swindale, N. Anatomical properties and physiological correlates of the intrinsic connections in cat area 18. *J. Neurosci.* **7**, 1428–1446 (1987).

42. Hung, C. P., Ramsden, B. M., Chen, L. M. & Roe, A. W. Building surfaces from borders in Areas 17 and 18 of the cat. *Vision Research* **41**, 1389–1407 (2001).

43. Orban, G. A., Kennedy, H. & Maes, H. Functional changes across the 17?18 border in the cat. *Exp Brain Res* **39**, (1980).

44. Olavarria, J. F. Non-mirror-symmetric patterns of callosal linkages in areas 17 and 18 in cat visual cortex. *J. Comp. Neurol.* **366**, 643–655 (1996).

45. Lu, H. D., Chen, G., Ts'o, D. Y. & Roe, A. W. A rapid topographic mapping and eye alignment method

using optical imaging in Macaque visual cortex. *NeuroImage* **44**, 636–646 (2009).

46. Chernov, M. M., Friedman, R. M. & Roe, A. W. Fiberoptic array for multiple channel infrared neural stimulation of the brain. *Neurophoton.* **8**, (2021).

47. Lu, H. D., Chen, G., Cai, J. & Roe, A. W. Intrinsic signal optical imaging of visual brain activity: Tracking of fast cortical dynamics. *NeuroImage* **148**, 160–168 (2017).

48. Lamme, V. A. F., Van Dijk, B. W. & Spekreijse, H. Organization of contour from motion processing in primate visual cortex. *Vision Research* **34**, 721–735 (1994).

49. Logothetis, N. K. *et al.* The effects of electrical microstimulation on cortical signal propagation. *Nat Neurosci* **13**, 1283–1291 (2010).

50. Bosking, W. H., Beauchamp, M. S. & Yoshor, D. Electrical Stimulation of Visual Cortex: Relevance for the Development of Visual Cortical Prosthetics. *Annu. Rev. Vis. Sci.* **3**, 141–166 (2017).

51. Movshon, J. A., Thompson, I. D. & Tolhurst, D. J. Spatial summation in the receptive fields of simple cells in the cat's striate cortex. *The Journal of Physiology* **283**, 53–77 (1978).

52. Oswalt, D. *et al.* Multi-electrode stimulation evokes consistent spatial patterns of phosphenes and improves phosphene mapping in blind subjects. *Brain Stimulation* **14**, 1356–1372 (2021).

53. Chen, R., Wang, F., Liang, H. & Li, W. Synergistic Processing of Visual Contours across Cortical Layers in V1 and V2. *Neuron* **96**, 1388-1402.e4 (2017).

54. Schultz, J. & Bulthoff, H. H. Parametric animacy percept evoked by a single moving dot mimicking natural stimuli. *Journal of Vision* **13**, 15–15 (2013).

55. Ramsden, B. M., Hung, C. P. & Roe, A. W. Real and Illusory Contour Processing in Area V1 of the Primate: a Cortical Balancing Act. *Cerebral Cortex* **11**, 648–665 (2001).

56. Jancke, D., Chavane, F., Naaman, S. & Grinvald, A. Imaging cortical correlates of illusion in early visual cortex. *Nature* **428**, 423–426 (2004).

57. Lamme, V. A. F., Van Dijk, B. W. & Spekreijse, H. Contour from motion processing occurs in primary visual cortex. *Nature* **363**, 541–543 (1993).

58. Rochefort, N. L., Buzás, P., Kisvárday, Z. F., Eysel, U. T. & Milleret, C. Layout of transcallosal activity in cat visual cortex revealed by optical imaging. *NeuroImage* **36**, 804–821 (2007).

59. Hunter, Z. R., Brysbaert, M. & Knecht, S. Foveal Word Reading Requires Interhemispheric Communication. *Journal of Cognitive Neuroscience* **19**, 1373–1387 (2007).

60. Blakemore, C., Diao, Y. C., Pu, M. L., Wang, Y. K. & Xiao, Y. M. Possible functions of the interhemispheric connexions between visual cortical areas in the cat. *The Journal of Physiology* **337**, 331–349 (1983).

61. Payne, B. R. Function of the corpus callosum in the representation of the visual field in cat visual cortex. *Vis Neurosci* **5**, 205–211 (1990).

62. Payne, B. R. & Siwek, D. F. The Visual Map in the Corpus Callosum of the Cat. *Cereb Cortex* **1**, 173–188 (1991).

63. Kennedy, H., Dehay, C. & Bullier, J. Organization of the callosal connections of visual areas v1 and v2 in the macaque monkey. *J. Comp. Neurol.* **247**, 398–415 (1986).

64. Cayce, J. M., Friedman, R. M., Jansen, E. D., Mahavaden-Jansen, A. & Roe, A. W. Pulsed infrared light alters neural activity in rat somatosensory cortex in vivo. *NeuroImage* **57**, 155–166 (2011).

65. Richter, C.-P. & Tan, X. Photons and neurons. *Hearing Research* **311**, 72–88 (2014).

66. Murphey, D. K., Yoshor, D. & Beauchamp, M. S. Perception Matches Selectivity in the Human Anterior

Color Center. *Current Biology* **18**, 216–220 (2008).

67. Kim, T. *et al.* Injectable, Cellular-Scale Optoelectronics with Applications for Wireless Optogenetics. *Science* **340**, 211–216 (2013).

68. Kim, A. *et al.* An Implantable Ultrasonically-Powered Micro-Light-Source (μLight) for Photodynamic Therapy. *Sci Rep* **9**, 1395 (2019).

69. Zhang, Y. *et al.* Battery-free, lightweight, injectable microsystem for in vivo wireless pharmacology and optogenetics. *Proc. Natl. Acad. Sci. U.S.A.* **116**, 21427–21437 (2019).

70. Ruiz, O. *et al.* Optogenetics through windows on the brain in the nonhuman primate. *Journal of Neurophysiology* **110**, 1455–1467 (2013).

71. Roe, A. W. BMI 2.0: Toward a technological interface with brainwide networks. *Neuron* **111**, 1687–1688 (2023).

72. Shi, S. *et al.* Infrared neural stimulation with 7T fMRI: A rapid in vivo method for mapping cortical connections of primate amygdala. *NeuroImage* **231**, 117818 (2021).

73. Yao, S. *et al.* Functional topography of pulvinar–visual cortex networks in macaques revealed by INS–fMRI. *J of Comparative Neurology* **531**, 681–700 (2023).

74. Armenta Salas, M. *et al.* Sequence of visual cortex stimulation affects phosphene brightness in blind subjects. *Brain Stimulation* **15**, 605–614 (2022).

75. Bosking, W. H. *et al.* Percepts evoked by multi-electrode stimulation of human visual cortex. *Brain Stimulation* **15**, 1163–1177 (2022).

76. Innocenti, G. Cellular aspects of callosal connections and their development. *Neuropsychologia* **33**, 961–987 (1995).

77. Coppola, D. M., White, L. E., Fitzpatrick, D. & Purves, D. Unequal representation of cardinal and oblique contours in ferret visual cortex. *Proc. Natl. Acad. Sci. U.S.A.* **95**, 2621–2623 (1998).

78. Watroba, L., Buser, P. & Milleret, C. Impairment of binocular vision in the adult cat induces plastic changes in the callosal cortical map. *Eur J of Neuroscience* **14**, 1021–1029 (2001).

79. Rockland, K. S. Anatomical organization of primary visual cortex (area 17) in the ferret. *J of Comparative Neurology* **241**, 225–236 (1985).

Figures

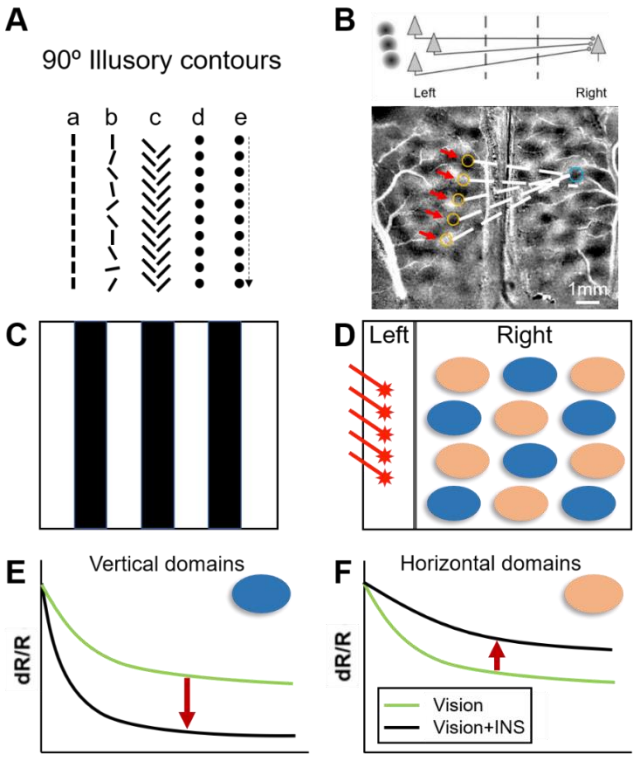

Figure 1. Experimental scheme. (A) Perception of 90º contours induced by higher order illusory contours. a. single orientation b. mixed orientation c. abutting line illusory contour d. aligned points e. sequential aligned points. (B) Upper: Schematic of 'high order projection' via callosal connection[22]. Below: Predicted activation in right hemisphere following stimulation of multiple aligned domains in left hemisphere. (C) Example of vertical grating or horizontal grating for visual stimulation. (D) "Vertical" INS applied at five points parallel to the vertical meridian in left hemisphere. Orientation-selective domains in right hemisphere mapped using optical imaging (OI); blue ovals: vertical domains, orange ovals: horizontal domains. (E & F) Schematic of expected OI response. Green lines: OI response curves for visual stimulation alone; black lines: response for vision + INS. Vertical INS added to visual stimulation (E) enhances grating response of vertical domains (downward red arrow) and (F) reduces grating response of horizontal domains (upward red arrow).

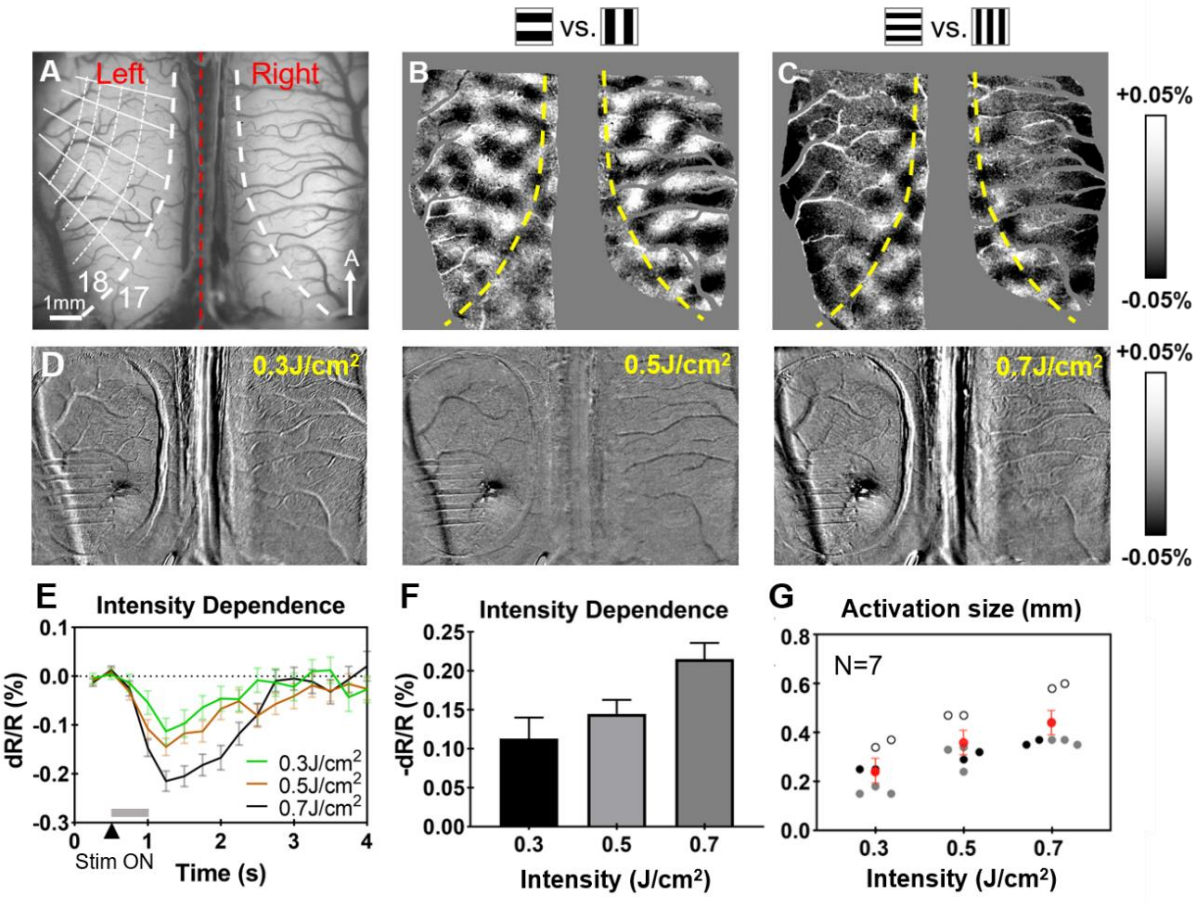

Figure 2. Procedure for determining the 17/18 border and intensity dependence of single fiber stimulation. (A) Vessel map of the cortex in the optical window, area 18 in both left and right brain are exposed and imaged at the same time. Red dashed line: midline; thick white dashed line: vertical meridian (VM); thin white dashed lines: iso-polar lines; thin white solid lines: iso-eccentricity lines. (B) OI response map of 'H' – 'V' visual stimulation with low spatial and high temporal (0.2 cyc per deg, 5Hz) frequency showing activation of area 18. (C) OI response map of 'H' – 'V' visual stimulation with high spatial and low temporal (0.5 cyc per deg, 2Hz) frequency showing activation of area 17. Yellow dashed lines mark the 17/18 border (VM). 20 trials per image. Optical imaging field of view: 10.5mm*8.7mm; scale bar: 1mm, A = anterior. Data from Cat 1. (D) Intensity dependence via a single fiber with the radiant exposure from 0.3-0.7 $J \cdot cm^{-2}$. (E-F) Time course (E), amplitude (F) of cortical response to INS stimulation in (D). 20 trials. (G) Diameter of the activation areas from 7 sessions of 3 cases. Black/gray/white circles: result from different cases. Red circles: average diameter across 3 cases (0.3 $J \cdot cm^{-2}$: 0.24mm, 0.5 $J \cdot cm^{-2}$: 0.35mm, 0.7 $J \cdot cm^{-2}$: 0.42mm). Error bar: SEM. N in (G) indicates number of sessions, one dot per session.

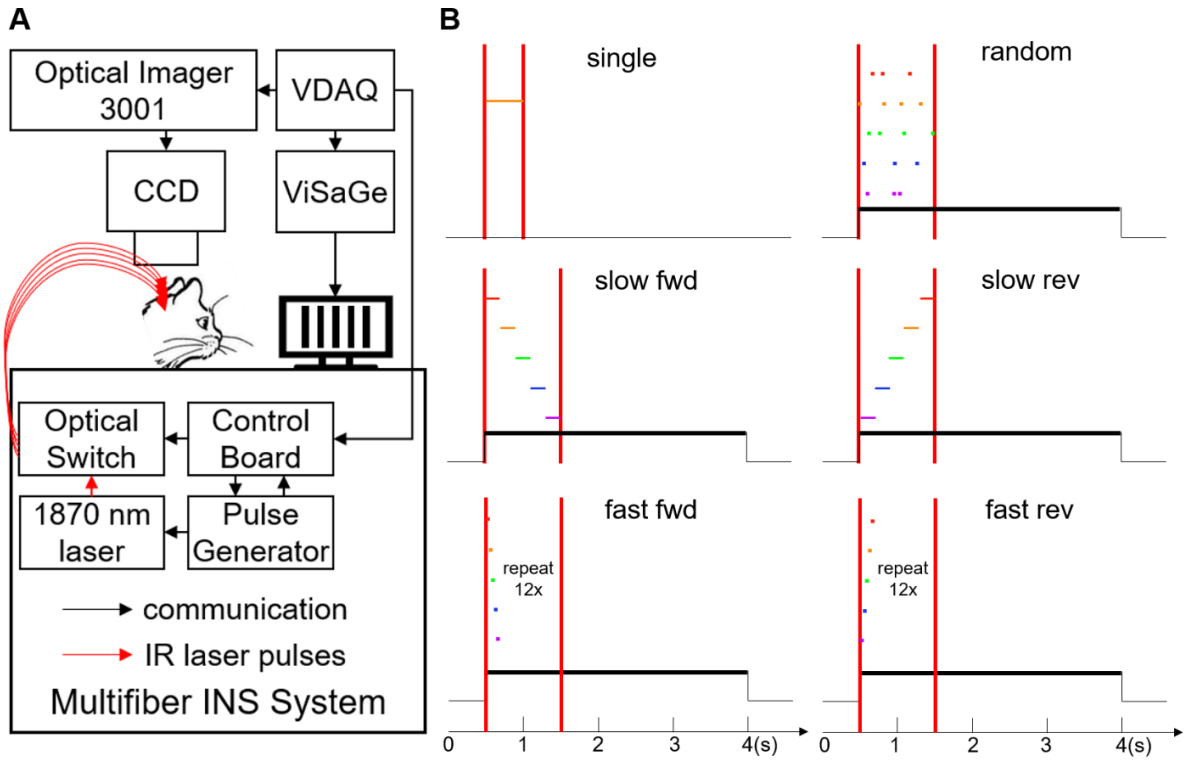

Figure 3. Experimental schematic and pulse sequence paradigms. (A) Schematic diagram of system combining OI, visual stimulation, and INS. See methods. (B) Time course for six INS conditions. single: 500ms pulse train applied to one optical fiber; random: 8 ms per fiber in random sequence for 1s total duration; slow fwd: 200 ms per fiber in sequence (1→5) for one cycle, 1.0s duration; slow rev: 200 ms per fiber in reverse sequence (5→1) for one cycle, 1.0s duration; fast fwd: 16 ms per fiber in sequence (1→5) for twelve cycles, 0.96s duration; fast rev: 16 ms per fiber in reverse sequence (5→1) for twelve cycles, 0.96s duration. All INS utilized pulse trains with pulse width of 250us at 200Hz; INS initiated coincident with visual stimulation 0.5s after the onset of OI data acquisition. OI acquisition 0 to 4s. Black line: visual stimulation ON. Vertical red lines: INS period.

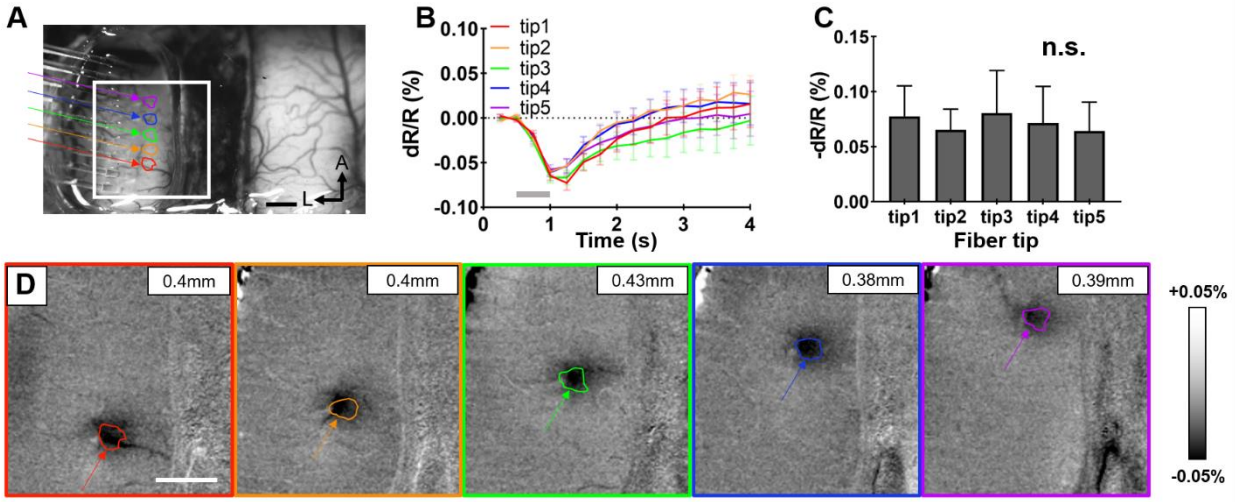

Figure 4. Single fiber INS activation in cat area 18. (A) Linear nine-fiber array placed on left hemisphere; scale bar: 1 mm; A = anterior, L = left. Single-pulse INS applied at five of nine fibers in the array. Colored arrows mark tips of the five fibers used (tips 1-5 from posterior to anterior). Colored ROIs mark areas of significant responses evoked by INS. The white box represents the area shown in (D). (B) Time course of OI signals in response to 0.3 $J \cdot cm^{-2}$ single-fiber INS for each ROI marked in (A). Gray bar indicates the duration of INS. Error bar: SEM. (C) Peak magnitude of OI signals plotted in (B); calculated p-values obtained from paired t-test show no statistically significant difference across all five fibers, error bars: SEM. (D) OI activation maps in response to INS show similar-sized focal activation areas. The diameter of activation size is within 500μm (Top right corner, activation region: $p<0.001$). INS: 1870 nm, 200 Hz, 0.3 $J \cdot cm^{-2}$, pulse width 250 μs, pulse train 500 ms, 50 trials. Scale bars: 1mm. Data from Cat 2.

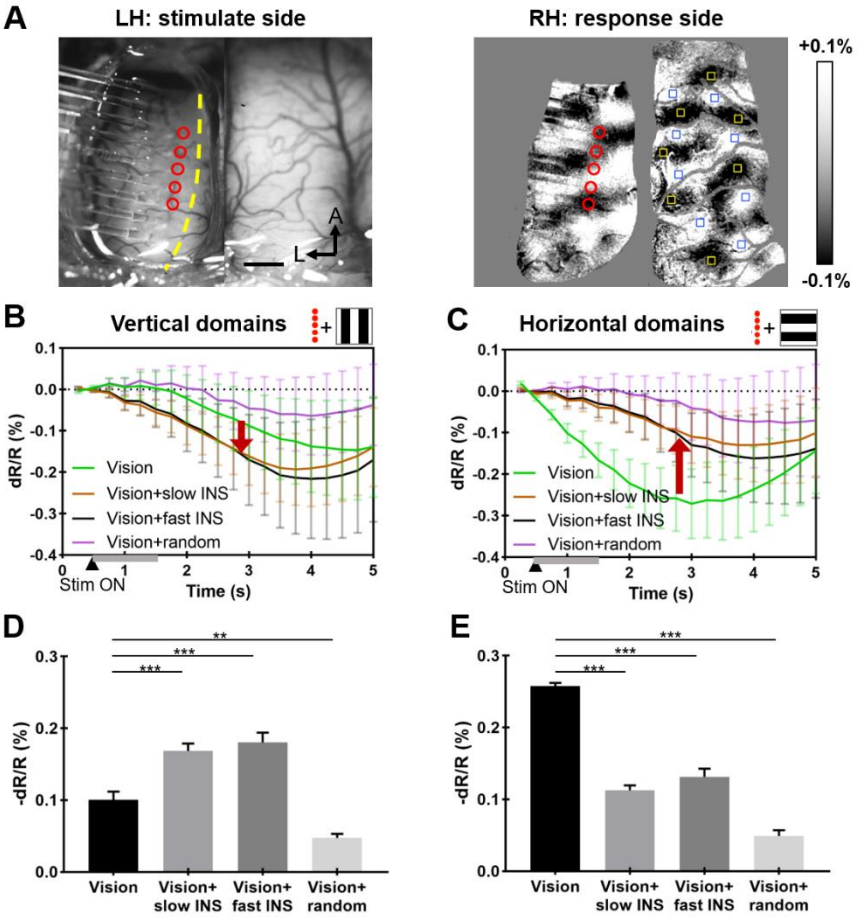

Figure 5. Orientation-selective response: vertically oriented INS fiber array (referred as 'vertical INS') in area 18 of left hemisphere. (A) Left panel: blood vessel map with nine-fiber linear array. Red circles: location of five fiber tips used. Right panel: orientation map generated by visual stimulation. Yellow boxes: center of ROIs in horizontal domains; blue boxes: center of ROIs in vertical domains. (B & C) Time course of OI signals for four different visual/INS stimuli combinations in vertical (B) and horizontal (C) domains. Gray bars from 0.5-1.5s: INS ON. Red arrows indicate that both slow (brown) and fast (black) vertical INS enhances visually evoked OI signals for vertical domains (B, down arrow) and suppress OI signals in horizontal domains (C, up arrow). Random condition (magenta) reduces OI response in both vertical (B) and horizontal domains (C). Error bar: SEM. (D & E) Averaged reflectance changes during 2.5 – 5s of the time courses in B & C. ***: P<0.001, **: P<0.01 (Welch's t-test, vision vs. vision + slow/fast/random INS). Error bars: SEM. INS: 1870 nm, 200 Hz, 0.3 J·cm^{-2}, pulse width 250 μs, pulse train 1 s, 15 trials. Scale bar in A: 1mm, A = anterior, L = Left. Data from Cat 2.

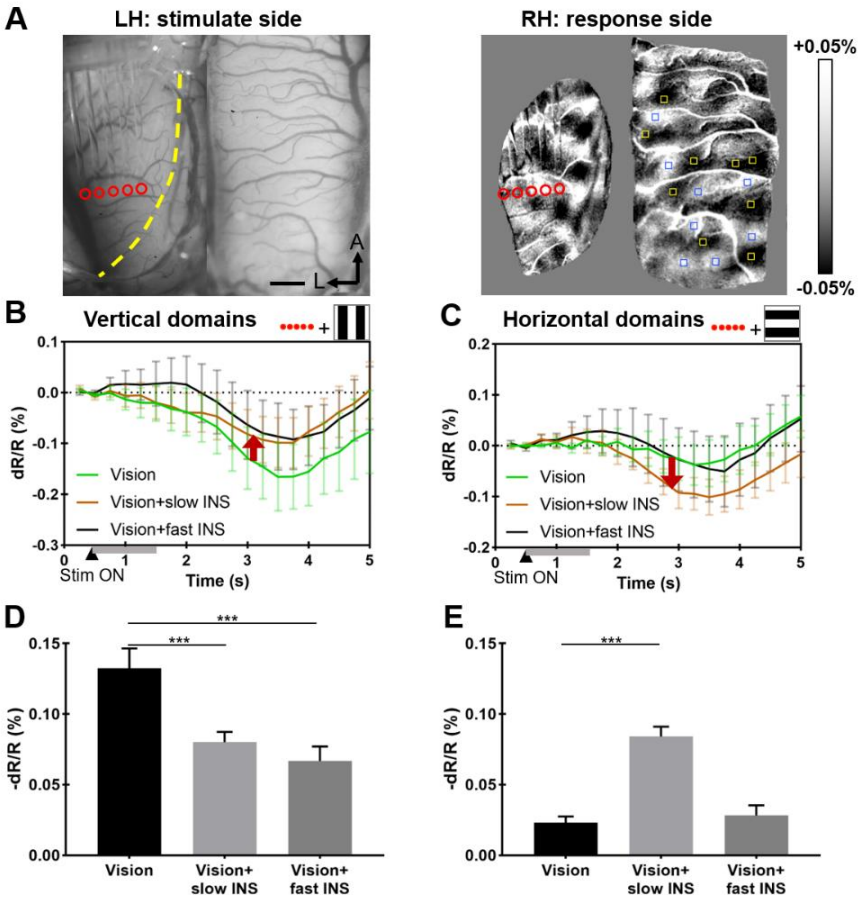

Figure 6. Orientation-selective response: horizontally oriented INS fiber array (referred as 'horizontal INS') in area 18 of left hemisphere. (A) Left panel: blood vessel map with five-fiber linear array. Red circles: location of five fiber tips used. Right panel: orientation map generated by visual stimulation. Yellow boxes: center of ROIs in horizontal domains; blue boxes: center of ROIs in vertical domains. (B & C) Time course of OI signals for three different visual/INS stimuli combinations in vertical (B) and horizontal (C) domains. Gray bars from 0.5-1.5s: INS ON. Red arrows indicate that both slow (brown, up arrow) and fast (black, down arrow) horizontal INS suppresses visually evoked OI signals for vertical domains (B) and slow horizontal INS enhances OI signals in horizontal domains (C). Error bar: SEM. (D & E) Averaged reflectance changes during 2.5 – 5s of the time courses in B & C. ***: P<0.001 (Welch's t-test, vision vs. vision + slow/fast INS). Error bars: SEM. INS: 1870 nm, 200 Hz, 0.3 J·cm^{-2}, pulse width 250 μs, pulse train 1 s, 10 trials. Scale bar in A: 1mm, A = anterior, L = Left. Data from Cat 3.

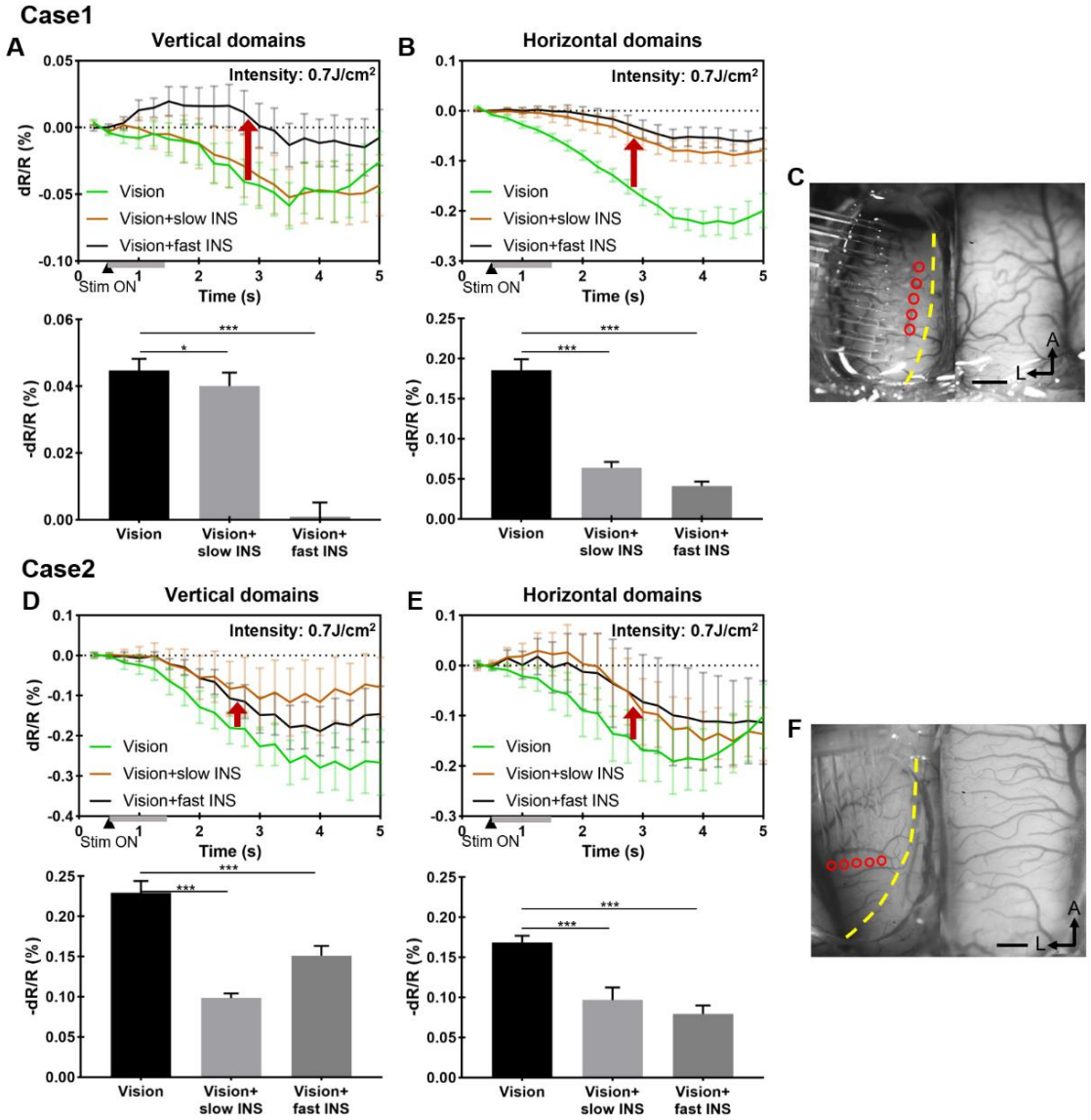

Figure 7. Reduction of OI response at high INS intensity. (A-B) Upper row is the time course of OI signal for three vision / INS stimulation conditions, measures at ROIs in vertical (A) and horizontal (B) domains shown in Fig.5A in manuscript. Bottom row is the average reflectance changes during 2.5-5s of the time courses in the upper row. ***: P<0.001, *: P<0.1 (Welch's t-test, vision vs. vision + slow/fast INS). (C) The location and direction of fiber array placement in case 1. (D-E) Upper row is the time course of OI signal for three vision / INS stimulation conditions (vertical, D vs. Horizontal, E domains shown in Fig.5A in manuscript). Bottom row is the average reflectance changes during 2.5-5s of the time courses in the upper row. (F) The location and orientation of the fiber array placement in case 2. Radiant exposure of INS in this figure: 0.7 $J \cdot cm^{-2}$. Gray bars from 0.5-1.5s: laser ON. Error bar: SEM.